

Metal–Organic Frameworks Stabilize Mono(phosphine)–Metal Complexes for Broad-Scope Catalytic Reactions

Takahiro Sawano,[†] Zekai Lin,[†] Dean Boures,[†] Bing An,[‡] Cheng Wang,[‡] and Wenbin Lin^{*,†,‡}

[†]Department of Chemistry, University of Chicago, 929 East 57th Street, Chicago, Illinois 60637, United States

[‡]Collaborative Innovation Center of Chemistry for Energy Materials, State Key Laboratory of Physical Chemistry of Solid Surfaces, Department of Chemistry, College of Chemistry and Chemical Engineering, Xiamen University, Xiamen 361005, P. R. China

S Supporting Information

ABSTRACT: Mono(phosphine)–M (M–PR₃; M = Rh and Ir) complexes selectively prepared by postsynthetic metalation of a porous triarylphosphine-based metal–organic framework (MOF) exhibited excellent activity in the hydrosilylation of ketones and alkenes, the hydrogenation of alkenes, and the C–H borylation of arenes. The recyclable and reusable MOF catalysts significantly outperformed their homogeneous counterparts, presumably via stabilizing M–PR₃ intermediates by preventing deleterious disproportionation reactions/ligand exchanges in the catalytic cycles.

Phosphine (PR₃)-ligated transition metal complexes have been essential to the development of organometallic chemistry and homogeneous catalysis, as exemplified by Wilkinson's catalyst RhCl(PPh₃)₃, Vaska's complex IrCl(CO)(PPh₃)₂, Crabtree's catalyst [Ir(pyridine)(cod)(PCy₃)₃]PF₆, and Grubb's catalyst (Ru(=CHPh)Cl₂(PCy₃)₂).¹ The number of coordinating phosphines control the metal's catalytic activity and selectivity by influencing its electronic and steric properties, as elegantly demonstrated in Buchwald's sterically hindered biaryl-phosphines which stabilize Pd–PR₃ complexes in C–X coupling reactions.² However, the number of phosphines on the metals often changes during the d⁶–d⁸ catalytic cycles for Rh and Ir catalysts because of their propensity to undergo disproportionation reactions/ligand exchanges. We surmised that catalytic site isolation in metal–organic frameworks (MOFs) could prevent deleterious ligand exchanges, thus stabilizing the mono(phosphine)–M intermediates in catalytic cycles (Figure 1), and constructed MOFs with M–PR₃ complexes for the efficient catalysis of a broad range of organic reactions.

MOFs have emerged as a new class of porous molecular materials for many potential applications such as gas storage, gas and liquid separations,³ chemical sensing,⁴ biomedical imaging,^{4a,5} and drug delivery.⁶ MOFs provide a highly tunable platform for designing single-site solid catalysts, for example, by incorporating orthogonal ligands to MOFs.⁷ Herein we report the first selective synthesis of (mono)phosphine–M complexes in MOFs (P₁-MOF·M, M = Rh and Ir) by taking advantage of the isolation of phosphine sites. The resulting P₁-MOF·M catalysts are highly active in the hydrosilylation of ketones and alkenes, the hydrogenation of alkenes, and the C–H borylation of arenes.

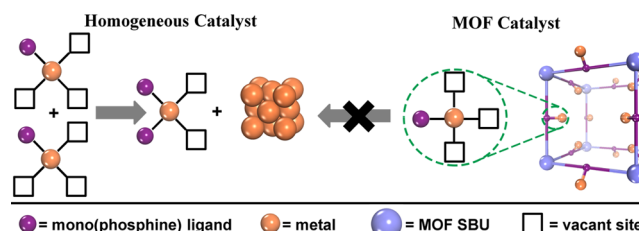


Figure 1. Catalytic site isolation stabilizes M–PR₃ complexes in MOFs by preventing disproportionation reactions/ligand exchanges to significantly enhance their activities.

We targeted a new P₁-MOF (**I**) with Zr-oxo SBUs and triarylphosphine-derived tricarboxylate (L) linkers, due to the stability of Zr–carboxylate bonds⁸ and the coordination incompatibility of hard Zr⁴⁺ ions and soft phosphine groups.^{9,10}

H₃L was synthesized in a 55% overall yield according to Scheme S1 (Supporting Information (SI)).¹¹ Heating a mixture of H₃L, ZrCl₄, and benzoic acid in DMF at 90 °C for 3 days afforded **I** in 34% yield as colorless needle crystals. Single crystal diffractions of **I** with synchrotron radiation failed to afford data sets of adequate resolution, presumably due to intrinsic disorders of the L ligands and framework distortion of **I**.

I has a solvent content of 83% by thermogravimetric analysis and exhibits a BET surface area of 471 m²/g by N₂ sorption measurements. Postsynthetic metalation of **I** with [RhCl(nbd)]₂ or [Ir(OMe)(cod)]₂ afforded P₁-MOF–Rh (**I**-Rh) or P₁-MOF–Ir (**I**-Ir) with controllable metal loadings. P₁-MOF–M catalysts of low metal loadings (15 mol % in **I**-Rh and 28 mol % in **I**-Ir), as determined by ICP-MS of digested P₁-MOF–M, were used for the catalytic reactions to maintain large open channels in the MOFs and facilitate diffusion of substrates and products. Powder X-ray diffraction (PXRD) indicated that the crystallinity of **I** was maintained in both **I**-Rh and **I**-Ir (Figure 2c).

Interestingly, fully metalated **I**-Rh and **I**-Ir gave satisfactory single crystal X-ray diffraction data sets under synchrotron radiation. Both **I**-Rh and **I**-Ir crystallize in the triclinic space group P $\bar{1}$ and adopt the llj topology by connecting the Zr₆(μ₃-O)₄(μ₃-OH)₄ SBU with 12 carboxylates from three L ligands. Unlike the UiO structure, in which all carboxylates bridge Zr

Received: June 16, 2016

Published: July 25, 2016

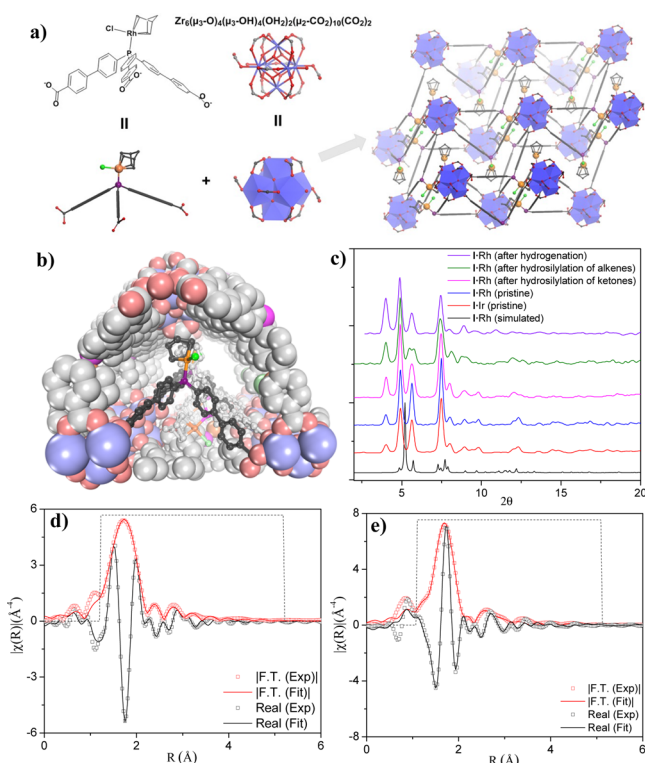


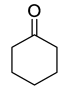
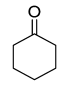
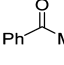
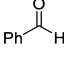
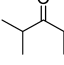
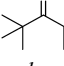
Figure 2. (a) Structures of I-Rh assembled from Zr-based SBUs and RhCl(nbd)(L) ligands. (b) Graphic presentation of the MCl(PR₃)(nbd) moieties in I-Rh as viewed along the (001) direction. (c) PXRD patterns of I-Rh simulated from the CIF file (black), freshly prepared I-Ir (red) and I-Rh (blue), and I-Rh recovered from hydrosilylation of ketones (pink) and alkenes (green), hydrogenation of alkenes (violet). (d) EXAFS spectra and fits of I-Rh in R space showing the magnitude of Fourier Transform (red hollow squares, red solid line) and real components (hollow squares, dashed line). The fitting range is 1.2–5.2 Å in R space (within the dashed lines). (e) EXAFS spectra and fits of I-Ir in R space showing the magnitude of Fourier Transform (red hollow squares, red solid line) and real components (hollow squares, dashed line). The fitting range is 1.1–5.1 Å in R space (within the dashed lines).

atoms,⁸ here, 10 of 12 carboxylates are bridging while the remaining two are monodentate, leaving each Zr-oxo SBU coordinating to two H₂O molecules. The void space was calculated to be 51.7% by PLATON. Rh coordinates to one Cl, one nbd, and one phosphine ligand in I-Rh (Figure 2a). The Ir coordination environment of I-Ir could not be determined from X-ray diffraction due to severe disorder.

We also investigated the metal coordination environments in I-Rh and I-Ir using X-ray absorption fine structure (XAFS) spectroscopy. We successfully used the crystal structure of RhCl(nbd)(PPh₃) to fit the EXAFS spectra of I-Rh and RhCl(nbd)(PPh₃) (Figure 2d).¹² We used a model of Ir coordinating to one methoxy, one bidentate cod, and one phosphine to fit the XAFS spectra of I-Ir and Ir(OMe)(cod)(PPh₃) (Figure 2e).¹³

I-Rh and I-Ir demonstrated excellent activity for several catalytic reactions. We first tested I-Rh for the hydrosilylation of ketones with silanes (Table 1).^{14,15} Reacting cyclohexanone and 1.5 equiv of triethylsilane in the presence of 0.0005 mol % I-Rh at rt for 20 h gave (cyclohexyloxy)triethylsilane in 36% yield (TON = 3600 h⁻¹, entry 1, Table 1).¹⁶ Prolonging the reaction to 140 h afforded the addition product in 93% yield,

Table 1. Hydrosilylation of Carbonyls Catalyzed by I-Rh

entry	carbonyl compound	silane	catalyst loading (mol% Rh)	time (h)	yield (%) ^a
1			0.0005	20	36
2		HSiEt ₃	0.0005	140	93
3			0.05	5	95
4 ^b			0.0005	20	0
5 ^c			0.0005	20	0
6		HSiMe ₂ Ph	0.005	60	90
7		HSiEt ₃	0.05	80	85
8		HSiEt ₃	0.01	140	90
9		HSiEt ₃	0.01	60	95
10		HSiEt ₃	0.01	80	94

^aIsolated yield. ^bRhCl(nbd)(PPh₃) was used. ^cRhCl(PPh₃)₃ was used. nbd = norbornadiene.

with a TON of 186 000 (entry 2, Table 1). A shorter reaction time (5 h) was needed when the catalyst loading increased to 0.05 mol % (entry 3, Table 1). In contrast, neither RhCl(nbd)(PPh₃) nor Wilkinson's catalyst gave any product under the same conditions (entries 4 and 5, Table 1). We believe that the site isolation of active catalysts in I-Rh is responsible for its higher catalytic activity because only one ligand coordinates to the Rh during the course of the reaction. Hydrosilylation proceeded for several kinds of silanes and ketones that we tested. We found that dimethylphenylsilane can be used for hydrosilylation (entry 6, Table 1). Hydrosilylation of acetophenone gave the corresponding alcohol in high yield (entry 7, Table 1). I-Rh also showed good activity for deriving primary alcohols from aldehydes (entry 8, Table 1). Sterically hindered ketones, such as diisopropyl ketone and di-*tert*-butyl ketone, could also be used in hydrosilylation, probably due to the open environment around the monophosphine-ligated Rh center (entries 9 and 10, Table 1).

We found that I-Rh is also highly active in the hydrosilylation of alkenes, a reaction frequently used in the industrial production of consumer goods and fine chemicals.¹⁷ Hydrosilylation of 1-octene with triethylsilane in the presence of 0.0001 mol % I-Rh at rt for 20 h selectively gave the anti-Markovnikov-type addition product in 34% yield (TON = 17 000 h⁻¹, entry 1, Table 2). Prolonging the reaction to 72 h afforded the addition product in 82% yield (TON = 820 000, entry 2, Table 2). The reaction time can be shortened to 4 h by increasing the catalyst loading to 0.05 mol % (entry 3, Table 2). The advantage of I-Rh over homogeneous controls was again demonstrated by comparison with RhCl(nbd)(PPh₃) or RhCl(PPh₃)₃; neither afforded any product under the same conditions (entries 4 and 5, Table 2). I-Rh-catalyzed hydrosilylation reactions work well for various silanes and alkenes.

Table 2. Hydrosilylation of Alkenes Catalyzed by I-Rh

$$R^1-CH=CH_2 + HSiR_3 \xrightarrow[THF, rt]{P_1-MOF \cdot Rh} R^1-CH_2-CH_2-SiR_3$$

entry	alkene	silane	catalyst loading (mol% Rh)	time (h)	yield (%) ^a
1			0.0001	20	34
2			0.0001	72	82
3		HSiEt ₃	0.05	4	81
4 ^b			0.0001	20	0
5 ^c			0.0001	20	0
6		HSiMe ₂ Ph	0.0005	40	82
7		HSi(OEt) ₃	0.005	40	84
8		HSiEt ₃	0.0005	40	84
9		HSiMe ₂ Ph	0.0005	40	83

^aIsolated yield. ^bRhCl(nbd) (PPh₃)₃ was used. ^cRhCl(PPh₃)₃ was used.

The hydrosilylation of 1-octene with dimethylphenylsilane and triethoxysilane gave 82% and 84% of the addition product, respectively (entries 6 and 7, Table 2). We could also hydrosilylate 1-decene and 6-chloro-1-hexene with I-Rh (entries 8 and 9, Table 2).

Many Rh-PR₃ compounds, including Wilkinson's catalyst, have been used to catalyze the hydrogenation of alkenes, but our MOF more effectively catalyzed hydrogenation of substituted alkenes at rt (Table 3). At 0.00005 mol % I-Rh loading, hydrogenation of 1-octene under 40 bar of H₂ yielded 22% of octane, giving a high TON of 440 000 (TOF = 17 000 h⁻¹, entry 1, Table 3). Under the same conditions, hydro-

Table 3. Hydrogenation of Alkenes by I-Rh

$$R^1-CH=CH-R^2 \xrightarrow[THF, rt, 40 h]{P_1-MOF \cdot Rh, H_2 (40 bar)} R^1-CH_2-CH_2-R^2$$

entry	alkene	catalyst	catalyst loading (mol% Rh)	yield ^a
1		I-Rh	0.00005	22 ^b
2		RhCl(PPh ₃) ₃	0.00005	0
3		I-Rh	0.0005	100
4 ^c		I-Rh	0.01	100
5		I-Rh	0.0005	98
6		I-Rh	0.0005	99
7		I-Rh	0.0005	99
8		I-Rh	0.1	99
9		I-Rh	0.001	81
10		RhCl(PPh ₃) ₃	0.001	0

^aIsolated yield. ^bNMR yield based on CH₃NO₂ as an internal standard. ^c6 h.

genation with Wilkinson's catalyst afforded no conversion (entry 2, Table 3). At 0.0005 mol % catalyst loadings, I-Rh afforded the reduction product in a quantitative yield (entry 3, Table 3). The reaction was completed in 6 h at a higher catalyst loading of 0.01 mol % (entry 4, Table 3).

The hydrogenation of alkenes by I-Rh has a broad substrate scope. With 0.0005 mol % catalyst loading, I-Rh converted styrene and cyclohexene to the corresponding alkanes in almost quantitative yields (entries 5 and 6, Table 3). Disubstituted alkenes, such as α -methylstyrene, were also good substrates (entry 7, Table 3). For the trisubstituted α -methyl stilbene, 0.1 mol % of I-Rh was needed to afford the reduction product in comparable yields, which might be due to slow diffusion of the large substrate through MOF channels (entry 8, Table 3). I-Rh displayed good activity for a tetrasubstituted alkene (entry 9, Table 3), while Wilkinson's catalyst¹⁸ showed no activity under the same reaction conditions (entry 10, Table 3).

I-Rh could be recovered and reused 9 to 19 times without any loss of activity in each of the above reactions (Schemes S2, S4, and S5, SI). We conducted several tests to demonstrate the heterogeneity of I-Rh. First, we showed that the PXRD of I-Rh recovered from each of the above reactions remained the same as that of freshly prepared I-Rh (Figure 2c). Second, we used ICP-MS to show that the amounts of Rh and Zr leaching into the supernatant during the hydrosilylation of cyclohexanone and 1-octene and hydrogenation of 1-octene were less than 1.3%/0.1%, 1.1%/0.03%, and 2.0%/0.17%, respectively. Finally, we observed that the removal of I-Rh from the reaction mixture after several hours stopped the hydrosilylation of cyclohexanone and the hydrogenation of 1-octene (Schemes S3 and S6, SI).

Direct C-H borylation of arenes is a powerful method for obtaining arylboronates directly from arenes.¹⁹ We tested I-Rh for the borylation reaction with B₂(pin)₂. In the presence of 0.1 mol % of I-Ir, benzene was borylated to give PhBPin in 84% yield at 90 °C for 40 h (TOF = 21, entry 1, Table 4).²⁰ The borylated product was obtained in 123% isolated yield with 0.2 mol % catalyst (entry 2, Table 4). Increasing the catalyst

Table 4. C-H Active Borylation of Arenes by I-Ir

$$C_6H_5-R + B_2(pin)_2 \xrightarrow[90^\circ C, 40 h]{P_1-MOF \cdot Ir} C_6H_4(B(pin))-R$$

entry	arene	product	catalyst loading (mol% Ir)	yield (%) ^a
1			0.1	84
2			0.2	123
3 ^b			4	118
4 ^c			0.1	13
5			0.2	120 (o:m:p = 9:63:28)
6			0.2	114 (o:m:p = 81:11:8)
7			0.2	117 (3:4 = 74:26)

^aIsolated yield based on B₂(pin)₂. ^b3 h. ^cIr(OMe)(cod)(PPh₃) was used. pin = pinacolate, cod = 1,5-cyclooctadiene.

loading to 4 mol % shortened the reaction time to 3 h (entry 3, Table 4). The homogeneous control, Ir(OMe)(cod)(PPh₃), gave only a 13% yield under identical conditions (entry 4, Table 4). We also tested I-Ir as a catalyst for the borylation of several kinds of substituted arenes. 0.2 mol % of I-Ir catalyzed the borylation of toluene to afford a mixture of borylated products in 120% yield (*o:m:p* = 9:63:28, entry 5, Table 4). The *ortho*-selective arene borylation was achieved using an arene with the carboxylate directing group (entry 6, Table 4). We found that the borylation of 1,2-dichlorobenzene occurred preferentially at the 3 positions (entry 7, Table 4). We then investigated the nature of Ir species involved in C–H borylation. EXAFS studies indicated the formation of five-coordinate Ir(PPh₃)(Bpin)₃(η²-COD) species upon treating I-Ir with an excess of B₂(pin)₂, suggesting the ability to maintain mono(phosphine) coordination on the Ir center during the catalytic cycle (Figure S10, Table S4). We demonstrated the heterogeneity of I-Ir with a reuse experiment (Scheme S7, SI), the similarity of PXRD patterns of I-Ir before and after borylation (Figure S14, SI), and by measuring the very low leaching of Ir (0.9%) and Zr (0.007%) during the borylation reaction.

In summary, we report the first example of a porous and crystalline Zr-MOF based on a triarylphosphine-derived tricarboxylate linker, and its postsynthetic metalation with Rh and Ir to afford single-site mono(phosphine)–M catalysts for the hydrosilylation of ketones and alkenes, the hydrogenation of alkenes, and the C–H borylation of arenes. The MOF catalysts not only showed superior activity to the corresponding homogeneous controls but also can be reused multiple times without any loss of catalytic activity. We believe that the ability to maintain mono(phosphine) coordination during the catalytic cycle in MOFs should afford interesting opportunities for the design of other highly active and selective catalysts for a broad range of organic reactions.

■ ASSOCIATED CONTENT

Supporting Information

The Supporting Information is available free of charge on the ACS Publications website at DOI: 10.1021/jacs.6b06239.

Crystallographic data for I-Rh (CIF)

Crystallographic data for I-Ir (CIF)

General experimental section; synthesis and characterization of ligands, and P₁-MOF; crystal structure figure of I-Rh; details of the XAFS experiments, fitting method and model; procedures for MOF-catalyzed reactions (PDF)

■ AUTHOR INFORMATION

Corresponding Author

*wenbinlin@uchicago.edu

Notes

The authors declare no competing financial interest.

■ ACKNOWLEDGMENTS

We thank the NSF (CHE-1464941) for financial support and C. Poon for experimental help. Single crystal diffraction studies were performed at ChemMatCARS (Sector 15), APS, Argonne National Laboratory (ANL). ChemMatCARS is principally supported by NSF/CHE-1346572 from the NSF Divisions of Chemistry (CHE) and Materials Research (DMR). XAFS data were collected at the APS at ANL on Beamline 10BM-B, supported by the Materials Research Collaborative Access

Team (MRCAT) and Sector 20. MRCAT operations are supported by the DOE and the MRCAT member institutions. Sector 20 operations are supported by the U.S. Department of Energy and the Canadian Light Source. Use of the APS, an Office of Science User Facility operated for the U.S. Department of Energy (DOE) Office of Science by ANL, was supported by the U.S. DOE (DE-AC02-06CH11357).

■ REFERENCES

- (1) (a) Hartwig, J. F. *Organotransition Metal Chemistry: from Bonding to Catalysis*; University Science Books: Sausalito, CA, 2010. (b) van Leeuwen, P. W. N. M. *Homogeneous Catalysis: Understanding the Art*; Kluwer Academic: Dordrecht, 2004.
- (2) Martin, R.; Buchwald, S. L. *Acc. Chem. Res.* **2008**, *41*, 1461–1473.
- (3) (a) Dincă, M.; Long, J. R. *Angew. Chem., Int. Ed.* **2008**, *47*, 6766–6779. (b) Rowsell, J. L. C.; Yaghi, O. M. *Angew. Chem., Int. Ed.* **2005**, *44*, 4670–4679.
- (4) (a) Liu, D.; Lu, K.; Poon, C.; Lin, W. *Inorg. Chem.* **2014**, *53*, 1916–1924. (b) Kreno, L. E.; Leong, K.; Farha, O. K.; Allendorf, M.; Van Duyne, R. P.; Hupp, J. T. *Chem. Rev.* **2012**, *112*, 1105–1125. (c) Cui, Y.; Yue, Y.; Qian, G.; Chen, B. *Chem. Rev.* **2012**, *112*, 1126–1162.
- (5) Lin, W.; Rieter, W. J.; Taylor, K. M. L. *Angew. Chem., Int. Ed.* **2009**, *48*, 650–658.
- (6) Rocca, J. D.; Liu, D.; Lin, W. *Acc. Chem. Res.* **2011**, *44*, 957–968.
- (7) (a) Gascon, J.; Corma, A.; Kapteijn, F.; Llabrés i Xamena, F. X. *ACS Catal.* **2014**, *4*, 361–378. (b) Yoon, M.; Srirambalaji, R.; Kim, K. *Chem. Rev.* **2012**, *112*, 1196–1231. (c) Ma, L.; Abney, C.; Lin, W. *Chem. Soc. Rev.* **2009**, *38*, 1248–1256. (d) Lee, J.; Farha, O. K.; Roberts, J.; Scheidt, K. A.; Nguyen, S. T.; Hupp, J. T. *Chem. Soc. Rev.* **2009**, *38*, 1450–1459.
- (8) Cavka, J. H.; Jakobsen, S.; Olsbye, U.; Guillou, N.; Lamberti, C.; Bordiga, S.; Lillerud, K. P. *J. Am. Chem. Soc.* **2008**, *130*, 13850–13851.
- (9) (a) Nuñez, A. J.; Shear, L. N.; Dahal, N.; Ibarra, I. A.; Yoon, J.; Hwang, Y. K.; Chang, J.-S.; Humphrey, S. M. *Chem. Commun.* **2011**, *47*, 11855–11857. (b) Redondo, A. B.; Morel, F. L.; Ranocchiaro, M.; van Bokhoven, J. A. *ACS Catal.* **2015**, *5*, 7099–7103.
- (10) (a) Bohnsack, A. M.; Ibarra, I. A.; Bakhmutov, V. I.; Lynch, V. M.; Humphrey, S. M. *J. Am. Chem. Soc.* **2013**, *135*, 16038–16041. (b) Falkowski, J. M.; Sawano, T.; Zhang, T.; Tsun, G.; Chen, Y.; Lockard, J. V.; Lin, W. *J. Am. Chem. Soc.* **2014**, *136*, 5213–5216. (c) Burgess, S. A.; Kassie, A.; Baranowski, S. A.; Fritzsche, K. J.; Schmidt-Rohr, K.; Brown, C. M.; Wade, C. R. *J. Am. Chem. Soc.* **2016**, *138*, 1780–1783.
- (11) Václavík, J.; Servalli, M.; Lothschütz, C.; Szlachetko, J.; Ranocchiaro, M.; van Bokhoven, J. A. *ChemCatChem* **2013**, *5*, 692–696.
- (12) Sparkes, H. A.; Brayshaw, S. K.; Weller, A. S.; Howard, J. A. K. *Acta Crystallogr., Sect. B: Struct. Sci.* **2008**, *64*, 550–557.
- (13) The model is derived from two crystal structures (CCDC number: 700005 and 1155618).
- (14) Díez-González, S.; Nolan, S. P. *Org. Prep. Proced. Int.* **2007**, *39*, 523–559.
- (15) Hamasaka, G.; Kawamorita, S.; Ochida, A.; Akiyama, R.; Hara, K.; Fukuoka, A.; Asakura, K.; Chun, W. J.; Ohmiya, H.; Sawamura, M. *Organometallics* **2008**, *27*, 6495–6506.
- (16) I-Rh with 56 mol% Rh loading (relative to phosphine equivalents) gave a 24% yield under the same reaction conditions.
- (17) (a) Marciniak, B. *Coord. Chem. Rev.* **2005**, *249*, 2374–2390. (b) Marciniak, B.; Guliński, J.; Urbaniak, W.; Kornetka, Z. W. *Comprehensive Handbook on Hydrosilylation*; Pergamon: Oxford, 2002. (c) Roy, A. K. *Adv. Organomet. Chem.* **2007**, *55*, 1–59.
- (18) Crabtree, R. *Acc. Chem. Res.* **1979**, *12*, 331–337.
- (19) Mkhali, I. A. I.; Barnard, J. H.; Marder, T. B.; Murphy, J. M.; Hartwig, J. F. *Chem. Rev.* **2010**, *110*, 890–931.
- (20) Kawamorita, S.; Ohmiya, H.; Hara, K.; Fukuoka, A.; Sawamura, M. *J. Am. Chem. Soc.* **2009**, *131*, 5058–5059.